Signatures of Spin Pairing in Chaotic Quantum Dots

S. Lüscher,[1] T. Heinzel,[1] K. Ensslin,[1] W. Wegscheider,[2,3] and M. Bichler[3]

[1]*Solid State Physics Laboratory, ETH Zürich, 8093 Zürich, Switzerland*
[2]*Institut für Angewandte und Experimentelle Physik, Universität Regensburg, 93040 Regensburg, Germany*
[3]*Walter Schottky Institut, TU München, 85748 Garching, Germany*

Coulomb blockade resonances are measured in a GaAs quantum dot in which both shape deformations and interactions are small. The parametric evolution of the Coulomb blockade peaks shows a pronounced pair correlation in both position and amplitude, which is interpreted as spin pairing. As a consequence, the nearest-neighbor distribution of peak spacings can be well approximated by a modified bimodal Wigner surmise, in which interactions are taken into account beyond the constant interaction model.

PACS numbers: 73.23.Hk, 02.40.Xx, 73.21.–b

Recently, the Coulomb blockade (CB) of electronic transport through quantum dots, defined in two-dimensional electron gases in semiconductor heterostructures, has been of considerable interest [1]. One reason is that such dots are model systems to investigate the interplay between chaos and electron-electron (e-e) interactions. Here, a key feature is the distribution of nearest-neighbor Coulomb blockade peak spacings (NNS), which random matrix theory [2] (RMT) predicts to follow a bimodal Wigner surmise $P(s)$ for a noninteracting quantum dot of chaotic shape, i.e.,

$$P(s) = \frac{1}{2}[\delta(s) + P^{\beta}(s)]. \qquad (1)$$

$P^{\beta}(s)$ is the Wigner surmise for the corresponding Gaussian ensemble; i.e., $\beta = 1$ for systems with time inversion symmetry (Gaussian orthogonal ensemble—GOE), and $\beta = 2$ when time inversion symmetry is broken (Gaussian unitary ensemble—GUE). The peak spacing s is measured in units of the average spin-degenerate energy level spacing $\Delta = 2\pi\hbar^2/m^*A$, where m^* denotes the effective mass, and A the dot area. The δ function in $P(s)$ takes the spin degeneracy into account. RMT further predicts the standard deviation for $P(s)$ to be $\sigma = 0.62$ for $\beta = 1$ and $\sigma = 0.58$ for $\beta = 2$, respectively [3].

The comparison to experimental data is made by applying the constant-interaction model [4,5], which allows one to separate the constant single-electron charging energy E_C from the fluctuating energies of the levels inside the dot. In disagreement with the predictions of RMT, the experimentally obtained NNS distributions are usually best described by a *single Gaussian* with enhanced values of σ [6–9]. The data thus look as if spin pairing were absent, although in Ref. [10], a spin pair has been observed in a chaotic dot. It should be noted that spin pairing has been clearly observed in quantum dots with a small number N of electrons ($N \lesssim 40$). The addition spectrum of such dots can be well explained with the energy spectrum of some model potential [11]. For larger N, such models fail and the dots are expected to be described by statistical models, such as RMT.

The apparent absence of spin pairing in quantum dots in the statistical regime and the different shape of $P(s)$ have triggered tremendous recent theoretical work. One possible explanation is the additional e-e interaction inside the dot [6,12–18], which lead to "scrambling" of the energy spectrum [10,19] and can be characterized by the interaction parameter r_s, defined as the ratio between the Coulomb interaction of two electrons at their average spatial separation and the Fermi energy [12,16–18]. It is theoretically expected that the NNS distribution becomes Gaussian due to e-e interactions [14] and that σ increases for $r_s \gtrsim 2$ [16,17]. However, all experiments so far have been carried out in a regime where an increase in σ is not expected, i.e., in samples with $0.93 \leq r_s \leq 1.35$ [6–8], with the exception of Ref. [9], where $r_s = 2.1$.

Gate-voltage induced shape deformations of the dot can modify the NNS distribution as well. The deformation can be described by a parameter x, which corresponds to the distance between avoided crossings induced by the deformation, measured in units of the CB peak spacing. For $x \approx 1$, the NNS distribution of partly uncorrelated energy spectra is measured, resulting again in a Gaussian shape with enhanced σ [20,21]. Whether shape deformations or interactions dominate the shape of the NNS distribution is not clear, although there is experimental evidence that $x < 1$ and interactions are more important [9,10].

Here, we report measurements on a quantum dot in which both shape deformations and r_s are reduced. We observe a pronounced pair correlation of both position and amplitude of the Coulomb blockade resonances, which is sometimes interrupted by kinks in the parametric evolution. The pairing is interpreted as a spin signature: the energies of two states belonging to the same spatial wave function with opposite spin differ by an average interaction energy $\bar{\xi}$, which fluctuates with a standard deviation of σ_{ξ}. The measured NNS distribution is fitted to a modified bimodal Wigner surmise, with $\bar{\xi}$ and σ_{ξ} as fit parameters.

The sample is a Ga[Al]As heterostructure with a two-dimensional electron gas (2DEG) 34 nm below the surface. The quantum dot is defined by local oxidation with an atomic force microscope [inset in Fig. 1(a)] [22]. The
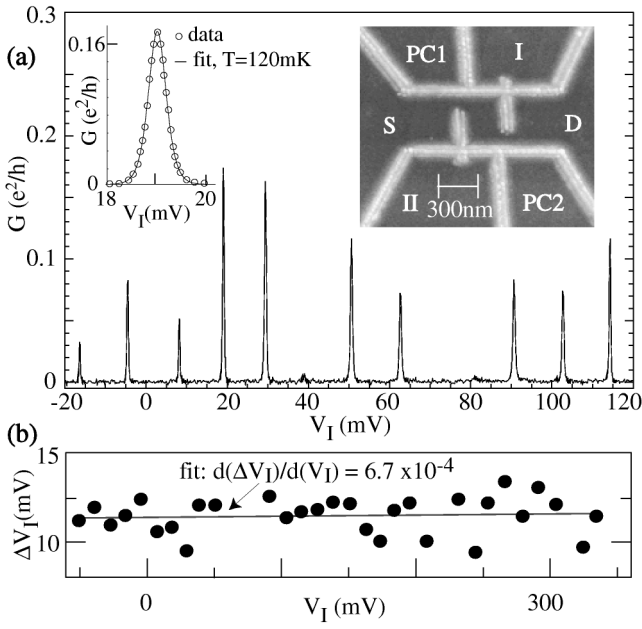
FIG. 1.   (a) Right inset: AFM picture (taken before evaporation of the top gate) of the oxide lines (bright) that define the dot, coupled to source (S) and drain (D) via tunnel barriers, which can be adjusted with the planar gates PC1 and PC2. Gates I and II are used to tune the dot. Main figure: conductance G as a function of V_I, showing Coulomb blockade resonances. Left inset: fit (line) to one measured CB peak (open circles); see text. (b) Linear fit (line) of a typical peak spacing ΔV_I as a function of V_I (dots) for a large range of V_I. The average peak spacing is almost constant, indicating small shape deformations.

lithographic dot area is 280 nm $\times$ 280 nm. The dot can be tuned by voltages applied to a homogeneous top gate and to the planar gates I and II. In order to reduce r_s as much as possible, we chose a heterostructure with a high electron density, further increased by a top gate voltage of $+100$ mV to $n_e = 5.9 \times 10^{15}$ m^{-2}. This results in $r_s = 0.72$, which is smaller than in all previous experiments; additional screening is provided by the top gate [23]. The sample was mounted in the mixing chamber of a ^{3}He/^{4}He-dilution refrigerator with a base temperature of 90 mK. The mobility of the cooled 2DEG was 93 m^2/V s. A DC bias voltage of 10 μV was applied across the dot, and the current is measured with a resolution of 500 fA. From capacitance measurements [5], we find an electronic dot area of 190 nm $\times$ 190 nm, $E_C = 1.25$ meV, and $\Delta = 200$ μeV.

The measurements have been carried out in the weak coupling regime, $\hbar\Gamma \ll k_B T \ll \Delta$. Here, Γ denotes the coupling of the dot to source and drain. The conductance G was measured as a function of the voltage V_I applied to the planar gate I [see inset in Fig. 1(a)]. Magnetic fields B applied perpendicular to the sample surface and V_{II} were used as parameters. The observed CB oscillations [Fig. 1(a)] are fitted to a thermally broadened line shape, i.e., $G(V_I) = G_{\max} \cosh^{-2}[\eta(V_I - V_{\max})/2k_B T]$ [4], yielding an electron temperature of $T = 120$ mK, as well as the positions and amplitudes of the peaks. Here, $\eta = $

0.11 eV/V is the lever arm, and $V_{\max}$ denotes the position of the peak maximum. Figure 1(b) shows typical peak spacings ΔV_I as a function of V_I. Compared to conventional dots defined by top gates [6–10,19], we find a much smaller variation of the average peak spacing as V_I is tuned, although the fluctuation of individual spacings is 15% of E_C. A linear fit gives a slope of $d(\Delta V_I)/d(V_I) = 6.7 \times 10^{-4}$. Hence, the capacitance between the dot and gate I varies only by 3% over the whole scan range, as compared to, for example, a factor of 3 in Ref. [7]. This indicates that tuning gate I or II predominantly changes the energy of the conduction band bottom, while the dot is only slightly deformed. By applying the method of Ref. [20] to a hard-wall confinement, we estimate $x \approx 0.15$ for our dot as a lower limit.

In Fig. 2(a), five consecutive CB peaks are shown as a function of B. A pronounced pair correlation of both amplitude and peak position is observed (peak b correlates with peak c, and peak d with peak e, respectively). We interpret this parametric pair correlation in terms of a model recently developed by Baranger et al. [24]. The constant interaction model is used to subtract E_c from the peak spacings. The remaining individual energy separations equal $\Delta/2$ on average and reflect the fluctuating level separations inside the quantum dot, which consist of two parts. We assume that two paired peaks belong to the same spatial wave function, labeled by i, of opposite spin, and are split by an interaction energy ξ_i, while the energy of consecutive states with different orbital wave functions differs by $\Delta_i - \xi_i$. This interpretation in terms of spin pairs is supported by measurements of the separation between strongly correlated peaks for $0 \leq B \leq 3$ T. We find a linear increase on average that corresponds to a g factor of about 0.45, which is very close to the bulk value of GaAs. Since the separations between the two levels of equal spin of spin pair i and $(i + 1)$, Δ_i, and possibly also ξ_i, vary as a function of B, levels may cross and the ground state of the dot can be either a singlet or a triplet state. Higher spin states are expected to be unlikely [14,25]. At the singlet-triplet transitions, kinks in the parametric peak evolution occur and the pair correlation is interrupted [24]. We can identify such kinks in our data, among other features. Figure 2(b) shows the amplitudes of peaks c, d, and e. The correlation between peaks d and e is very strong around $B = 0$. For 0.4 T $< B <$ 0.61 T, this correlation is interrupted, while the amplitudes of peaks c and e are correlated instead. In this regime, correlated kinks in the evolution of peaks c and d are observed [Fig. 2(c)]. In Fig. 2(d), a possible corresponding scenario for the parametric dependence of energy levels is sketched: (left) two avoided crossings occur between level pair i and level pair $i + 1$. This leads to the position of peaks c, d, and e as sketched in Fig. 2(d), right, corresponding to the difference in energy upon changing the electron number in the dot. Consequently, positions and amplitudes of peaks c and e should be correlated in 0.4 T $< B <$ 0.61 T, as observed. Note that this correlation is interrupted around $B = 0.5$ T,
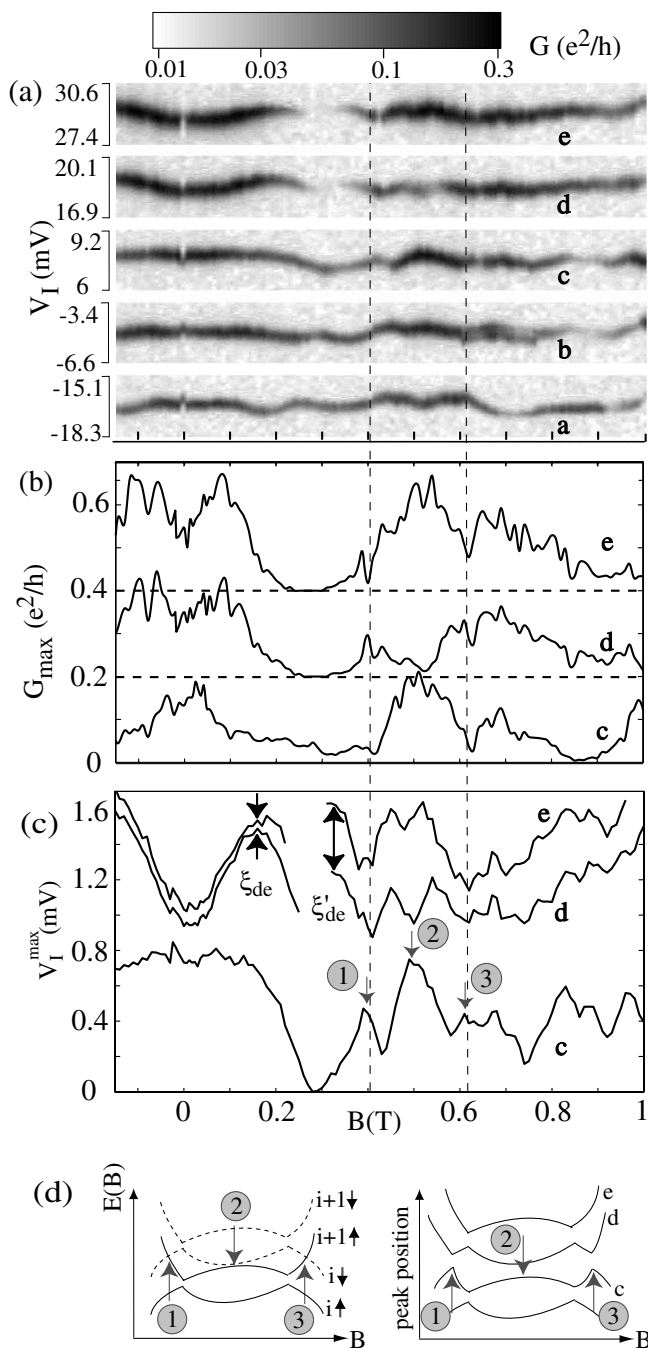
FIG. 2. (a) Logarithmic grayscale plot of parametric variations in a magnetic field B for five consecutive CB peaks. A pair correlation in peak position amplitude is observed, which is interrupted in certain ranges of B, for example, in the region between the dashed lines. (b) Parametric amplitudes for peaks c, d, and e, offset by $0.2e^2/h$ each. The correlation between peaks d and e is lost in 0.4 T $< B < 0.6$ T, and e correlates with c instead. (c) The corresponding position of the peak maxima. The traces are offset for clarity. At magnetic fields labeled by 1 and 3, kinks in the peak position occur, while the separation between peaks d and e jumps across the region of suppressed amplitude from ξ_{de} to ξ'_{de}. (d) Scheme of a possible double anticrossing between spin-paired level i and $i + 1$ (left, the black arrows indicate the spin), which could lead to the observed structure in the correlation for peaks c, d, and e (right).

possibly due to the influence of another energy level. We emphasize that this kink structure, i.e., a double-anticrossing between two spin pairs, is the dominant one for all peak evolutions. This fact does not depend on the cooldown cycle.

Also, ξ_{de} is not constant over the full range of B. While $\xi_{de} \approx 0.05\Delta$ for $B < 0.22$ T, the positions of peaks d and e are not detectable in 0.22 T $< B < 0.32$ T, since their amplitudes vanish. As the peaks reappear, ξ_{de} has jumped to $\xi^*_{de} \approx 0.25\Delta$. We speculate that possibly a level crossing has occurred in the regime where the amplitudes are suppressed, and hence for $B < 0.22$ T, a different level pair is at the Fermi energy than for $B > 0.32$ T. Although ξ fluctuates as B is varied, a systematic change of ξ with B cannot be clearly detected for $B < 1$ T, which indicates that Zeemann splitting is smaller than the parametric fluctuations in this regime. From the data of Fig. 2, we estimate the average interaction energy to $\overline{\xi} \approx 0.5\Delta$ by averaging over all peak pairs in their correlated regions. Baranger *et al.* have estimated $\overline{\xi} \approx 0.6\Delta$ for $r_s = 1$. Hence, our findings are in rough agreement with existing theory, while we are not aware of a theoretical prediction for σ_ξ. From the above phenomenology, we conclude that for dots with stronger shape deformations, and hence more level crossings, or in dots with larger r_s (and thus larger $\overline{\xi}$), the spin pairing is frequently interrupted and difficult to detect. This is possibly the reason why spin pairing has not been observed in the earlier experiments [6–9].

We proceed by discussing the effect of spin pairing on the NNS distributions. In Fig. 3, the measured histograms of the normalized NNS distributions for GOE (a) and GUE (b) are shown. Each individual V_I sweep contains 15 CB resonances in the low coupling regime. The ensemble statistics have been obtained by measuring $G(V_I)$
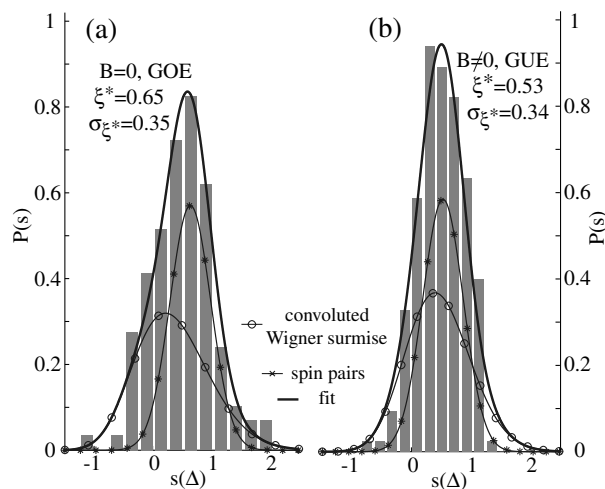

FIG. 3. Measured NNS distributions (gray bars) for $B = 0$ (a) and $B \neq 0$ (b). The bold solid curves are the fits to $P^\beta_{\text{int}}(\overline{\xi^*}, \sigma_{\xi^*})$, with the fit results as indicated in the figure (see text). Also drawn are the two components of P^β_{int}, i.e., the Gaussian distribution of separations between spin pairs, and its convolution with the corresponding Wigner surmises.

and by either changing the magnetic flux by one flux quantum $\phi_o = \frac{h}{e}$ through the dot (GUE) or stepping V_{II} in units of one CB period (GOE), which corresponds to the autocorrelation voltage for the peak amplitudes [10] in our sample. The total number of peak spacings used is 120 for GOE, and 210 for GUE, respectively. The individual level spacings s in units of Δ are obtained by using the fit of Fig. 1(b); its expectation value is $\overline{s} = 0.5$. Both histograms are asymmetric and show no evident bimodal structure. By including the effect of spin pairing into the statistics, however, we can interpret them as bimodal distributions, modified by (i) The δ function in the noninter-

acting NNS distribution $P(s)$ with the expectation value of $\overline{s_\delta} = 0$ [Eq. (1)] is shifted to $\overline{s_\delta} = \overline{\xi^*}$ and, as a reasonable assumption [26], broadened according to a Gaussian distribution with the standard deviation σ_{ξ^*}. Here, ξ^* denotes the interaction energy in units of Δ. (ii) Since one level of a spin pair i is shifted upwards in energy by ξ_i, the separation between the upper level of spin pair i and the lower level of pair $(i + 1)$ is given by $\Delta_i - \xi_i$. Consequently, $P^\beta(s)$ in Eq. (1) is shifted to $\overline{s_{P\beta}} = 1 - \overline{\xi^*}$ and convoluted with the Gaussian distribution function of ξ^*.

Combining these two components, the modified NNS distribution reads

$$P^\beta_{\text{int}}(\overline{\xi^*}, \sigma_{\xi^*}) = \frac{1}{\sqrt{2\pi}\,\sigma_{\xi^*}} \left\{ \exp\left[-\frac{(s - \overline{\xi^*})^2}{2\sigma_{\xi^*}^2} \right] + \exp\left[-\frac{s^2}{2\sigma_{\xi^*}^2} \right] \times P^\beta(s + \overline{\xi^*}) \right\}. \tag{2}$$

Here, "$\times$" denotes the convolution. Since Δ is determined by the dot size and the material parameters, we can fit $P^\beta_{\text{int}}(\overline{\xi^*}, \sigma_{\xi^*})$ to the measured NNS distribution with the two fit parameters $\overline{\xi^*}$ and σ_{ξ^*} (Fig. 3). We obtain $\overline{\xi^*} = 0.65$ and $\sigma_{\xi^*} = 0.35$ for GOE, as well as $\overline{\xi^*} = 0.53$ and $\sigma_{\xi^*} = 0.34$ for GUE. Hence, we find that $\overline{\xi}$ is higher for GOE than for GUE, which is in agreement with the theoretical prediction [24]. The fluctuation of $\overline{\xi^*}$ is found to be independent of the Gaussian ensemble and does not vary continuously with B within experimental accuracy. We emphasize that here, σ_{ξ^*} is an empirical fit parameter that includes not only the fluctuations of the spin splitting, but also other contributions, in particular, the Zeemann splitting and states with a total spin larger than $1/2$ (i.e., we have neglected situations in which $\xi_i > \Delta_i$). Hence, σ_{ξ^*} can be regarded only as an upper limit for the fluctuation of the interaction energy.

More experiments as well as theoretical work are necessary in order to get a more complete understanding of the fluctuations in the spin splitting.

In summary, we have observed spin pairing effects in a—compared to dots investigated in earlier experiments—rigid quantum dot with reduced electron-electron interactions. The spin pairing persists as a magnetic field is varied but is interrupted by kinks as well as other structures in the parametric evolution of the Coulomb blockade peaks. We have extracted the average interaction energy between states of identical spatial wave functions but opposite spin. Furthermore, we explain the measured distributions of nearest-neighbor spacings as being composed of the two branches of a modified, bimodal Wigner-Dyson distribution, which takes spin splitting and its fluctuation into account.

[1] For a review, see L. P. Kouwenhoven *et al.,* in *Mesoscopic Electron Transport,* edited by L. P. Kouwenhoven,
G. Schön, and L. L. Sohn, NATO Advanced Study Institutes, Ser. E, Vol. 345 (Kluwer, Dodrecht, The Netherlands, 1997), pp. 105–214.
[2] M. L. Mehta, *Random Matrices* (Academic Press, London, 1991).
[3] C. W. J. Beenakker, Rev. Mod. Phys. **69**, 731 (1997).
[4] C. W. Beenakker, Phys. Rev. B **44**, 1646 (1991).
[5] M. A. Kastner, Rev. Mod. Phys. **64**, 849 (1992).
[6] U. Sivan *et al.,* Phys. Rev. Lett. **77**, 1123 (1996).
[7] F. Simmel *et al.,* Europhys. Lett. **38**, 123 (1997).
[8] S. R. Patel *et al.,* Phys. Rev. Lett. **80**, 4522 (1998).
[9] F. Simmel *et al.,* Phys. Rev. B **59**, R10 441 (1999).
[10] S. R. Patel *et al.,* Phys. Rev. Lett. **81**, 5900 (1998).
[11] See, for example, S. Tarucha *et al.,* Phys. Rev. Lett. **77**, 3613 (1996); R. C. Ashoori *et al.,* Phys. Rev. Lett. **71**, 613 (1993).
[12] R. Berkovits and B. L. Altshuler, Phys. Rev. B **55**, 5297 (1997).
[13] Y. M. Blanter *et al.,* Phys. Rev. Lett. **78**, 2449 (1997).
[14] R. Berkovits, Phys. Rev. Lett. **81**, 2128 (1998).
[15] A. Cohen *et al.,* Phys. Rev. B **60**, 2536 (1999).
[16] P. N. Walker *et al.,* Phys. Rev. Lett. **82**, 5329 (1999), and references therein.
[17] K.-H. Ahn *et al.,* Phys. Rev. Lett. **83**, 4144 (1999), and references therein.
[18] Y. Alhassid *et al.,* cond-mat/9909066, and references therein.
[19] D. R. Stewart *et al.,* Science **278**, 1784 (1997).
[20] G. Hackenbroich *et al.,* Phys. Rev. Lett. **79**, 127 (1997).
[21] R. O. Vallejos *et al.,* Phys. Rev. Lett. **81**, 677 (1998).
[22] R. Held *et al.,* Appl. Phys. Lett. **75**, 1134 (1999); S. Lüscher *et al., ibid.* **75**, 2452 (1999).
[23] By magnetotransport measurements in the quantum Hall regime [following the technique described in P. L. McEuen *et al.,* Phys. Rev. B **45**, 11 419 (1992)], we have determined the magnetic field at which the filling factor inside equals 2, and we estimate the electron density inside the dot to 4.35×10^{15} m^{-2}. This corresponds to an effective r_s of 0.85. However, as a simple image charge calculation reveals, the top gate reduces r_s inside the dot to ≈ 0.64 only.
[24] H. U. Baranger *et al.,* Phys. Rev. B **61**, R2425 (2000).
[25] I. L. Kurland *et al.,* cond-mat/0005424.
[26] H. U. Baranger (private communication).